Limiting the rebound effects when utilising flexibility from heat pumps using an adaptive heat pump controller

Energy Conversion and Management 350 (2026) 120956

Contents lists available at ScienceDirect

Energy Conversion and Management

journal homepage: www.elsevier.com/locate/enconman

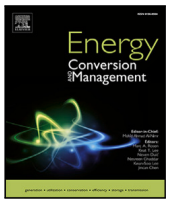

Research paper

Limiting the rebound effects when utilising flexibility from heat pumps using an adaptive heat pump controller

Sindhu Kanya Nalini Ramakrishna *, Torbjörn Thiringer, Peiyuan Chen

Division of Electric Power Engineering, Chalmers University of Technology, Gothenburg, 41296, Sweden

ARTICLE INFO

Keywords:
Heat pumps
Flexibility
Rebound power
Cold load pickup effects

ABSTRACT

Supporting power systems in severe power deficit conditions using flexibility from houses equipped with heat pumps is a powerful resilience action. However, the rebound effect of using flexibility has large negative cold load pick-up effects while restoring indoor temperatures to normal conditions. Even if the electric heaters in heat pumps are blocked, the standard heat pump controller will not operate fully desirable, leading to a large surplus rebound power consumption. The contribution of this article lies in proposing an adaptive heat pump controller to limit this effect. The proposed controller provides estimates of water supply temperatures to deliver maximum heat at various indoor temperatures during indoor temperature recovery.

The Swedish power system with a maximum consumption of 20–25 GW is used as a reference case. Here, at −5 °C outside temperature, approximately 1.9 GW is required to maintain indoor temperatures around 20 °C, in 44% of single-family houses. The power system can be relieved of 1.9 GW for 7 h and 650 MW for the next 10 h, with the consequence that the indoor temperatures drop to 15 °C. During the indoor temperature recovery to 20 °C, which takes 20 h, using the proposed controller, the maximum rebound power is limited to 2.6 GW compared to 3.9 GW using the standard controller. Thus, achieving a 33% reduction in peak power.

1. Introduction

The peak load period occurs during winter in northern European countries such as Sweden. This situation may become challenging during the loss of a major generation unit, combined with limitations in the transmission system for importing power, over a range of a few hours. Cyber attacks can inflict this [1] leading to severe power deficit conditions. Using the flexibility of heating systems equipped with heat pumps by compromising thermal comfort can be an alternative way of addressing this challenge [2,3]. Thus, flexibility from the aggregation of heat pumps in single family houses can be used as a valuable resource to support the power grid during such severe power shortages. In this study, flexibility is defined as a reduction in the electric power consumption of a heat pump, relative to the electric power consumption of the same heat pump while maintaining 20 °C in a house.

Taking Sweden as an example, the focus is specifically on single-family houses, since about 1.3 million out of 2 million houses use electricity for heating [4] and a majority of them are equipped with heat pumps. Looking into the future, variable speed heat pumps (VSHPs) are today dominating new installations and will thus in the future dominate also in the total installations. Hence, single-family houses equipped with VSHPs are considered for the analysis. However, using heat pumps to support the grid by compromising thermal comfort, during severe power deficit conditions, will have rebound effects [5], which takes place when restoring indoor temperature to normal conditions. The time during which the indoor temperature is restored to normal conditions is termed a recovery period in this article. These effects are substantial when today's control structure is used. Thus, the main objective of this study is to limit the rebound effect during the recovery period.

McKenna and Keane [6] confirms that participation of thermostatically controlled loads (TCL) in dynamic pricing schemes leads to cold load pickup (CLPU) effects, which are typically witnessed during network restoration after extended periods of outages. CLPU is a phenomenon in which there is a sudden increase in the load, followed by an eventual reduction to a value seen during pre-outage conditions. The increase in load is several times higher compared to the pre-outage conditions and is usually caused by TCLs such as refrigerators, freezers, air conditioners, electric boilers, electric radiators, and heat pumps [7]. Thus, heat pumps after having provided flexibility during the recovery period have significant CLPU effects. With this background, a literature review on CLPU effects is presented next.

There are several valuable articles dealing with the characterisation of the CLPU phenomenon to make informed decisions while restoring distribution feeders after power outages. For example, Schneider

* Corresponding author.
E-mail address: kanya@chalmers.se (S.K. Nalini Ramakrishna).

https://doi.org/10.1016/j.enconman.2025.120956
Received 26 September 2025; Received in revised form 6 December 2025; Accepted 14 December 2025

Nomenclature

Q_{heat}	Actual value of the heat delivered considering the limitations in the radiators and the heat pump.	T_{supply}	Radiator water supply temperature.
Q_{heat}^{*}	Reference value of the heat considering limitations in radiators.	ΔT	Temperature difference between supply and return temperature in radiators.
Q_{heat}^{**}	Reference value of the desired heat.	U_{value}	Heat transfer coefficient of the house.
T_{amb}	Outdoor ambient temperature.	$\hat{T}_{return}$ *	Estimated value of the return temperature in the heat emitters.
T_{cond}^{*}	Estimated condenser temperature of the heat pump.	$\hat{T}_{supply}$ *	Estimated value of the desired supply temperature in the heat emitters.
T_{return}	Radiator water return temperature.	$\hat{T}_{supply,maxheat}$ *	Estimate of supply temperature for delivering maximum heat considering limitations in radiators and the heat pump.
T_{room}	Room temperature.	$\hat{T}_{supply,rad}$ *	Estimated value of supply temperature desired in the radiators.
T_{room}^{*}	Room temperature reference.		
T_{source}	Source temperature of the heat pump.		

et al. [8] presents a method for evaluating the CLPU effects of heat pumps using multi-state models. Bu et al. [9] proposes a data-driven approach to estimate CLPU demand at the feeder level as well as at the customer level. A computationally efficient analytical method to quantify the CLPU demand is proposed in [10]. A general load modelling expression to estimate the CLPU demand is presented in [11]. Mortensen and Haggerty, [12] demonstrates the consistency of different mathematical models used to study CLPU effects, through simulations.

There are also beneficial articles on load restoration in distribution systems, involving CLPU loads. For example, Song et al. [13] deals with time-dependent CLPU effects, by accounting for the operating state evolution of TCLs. Ucak and Pahwa [14] deals with minimising the total restoration time, accounting for the loading limits of the transformer and CLPU effects. The significance of including CLPU effects in load restoration actions, leading to improved reliability of the distribution system, is demonstrated in [15]. Li et al. [16] proposes a stochastic decision-dependent service restoration, accounting for the relationship between the duration of the outage and the CLPU effect. A new variant of the typical CLPU model is proposed in [17]. A multi-objective algorithm including CLPU effects, to optimise load recovery is presented in [18]. In Menazzi et al. [19], a data-driven approach for load restoration is proposed for a system involving distributed energy resources and loads with CLPU effects. Qin et al. [20] deals with the resilience-driven restoration scheme using an enhanced situational awareness tool. This tool, among many other aspects, includes the estimation of the CLPU demand.

In the articles dealt with in [8–20], exponential, delayed exponential, and time-dependent models are used to represent CLPU effects. These models are based on the fact that the fixed speed or the on–off type of TCLs is considered, since the CLPU effect is a consequence of losing the load diversity among TCLs. Today, modern VSHPs are dominating new installations strongly, and they will soon dominate the accumulated installations. To sum up, the rebound effect following a power system support event using VSHPs is a very important scientific gap to fill.

Furthermore, in the above literature the focus is mainly on staggered load restoration involving loads with CLPU characteristics, in a distribution network after power outages. Additionally, the thermal dynamics involving the heat pump and indoor temperature is rarely addressed in the literature except in Schneider et al. [8]. In Schneider et al. [8] although the dynamics of indoor temperature is taken into account, the heat pump model is of fixed speed type and the heat pump model is not discussed in detail. Consequently, a proposal for a controller to limit rebound power at the component level of a heat pump, considering the dynamics of indoor temperature, is today missing in the literature and forms an important research gap to fill. The summary of this literature review is shown in Table 1.

With this background, this article contributes with the following

- A new heat pump control strategy is proposed to limit the CLPU effect at the component level, and its advantage over the standard controller is demonstrated.
- Quantification of electric power consumption as a function of time during flexibility and recovery periods, for various temperature reductions, accounting for different house characteristics and different types of modern VSHPs such as ground source and air source heat pumps. These results help to make informed decisions on load management while balancing power systems with limited generation and importing capacity, which will be a key feature in increasing grid resilience in the future.

The structure of this article is as follows. Section 2 deals with the mathematical modelling of the house, the heat pump and the controller to reduce the rebound effect of using flexibility. Section 3 deals with the data used for modelling various aspects dealt with in Section 2. Finally, results, discussions, and conclusions are dealt with in Sections 4 and 5, respectively.

2. Method

2.1. Thermal model for estimating the indoor temperature of houses equipped with heat pumps

The thermal model of a house equipped with a heat pump, accounting for the 'U_{value}', time constant, water-based radiators, a heat recovery unit followed by heat losses due to infiltration, and ventilation is modelled in detail in this article as described in [21].

The performance of heat pumps is estimated using a vapour compression heat pump cycle. In addition, performance with enhanced vapour injection, which is a new feature since some years, is estimated as detailed in [22]. An illustrative overview of the modelling aspects considered is schematically represented in Fig. 1.

This figure shows a house equipped with a heating system that involves radiators and a heat pump, a heat recovery unit, and heat losses to the outdoor environment.

2.2. Standard weather compensated control for heat pump

The standard weather compensated control for a heat pump is based on the heating demand in a house and does not include the maximum heat delivering capability of the heat pump. The details of this type of controller can be found in Appendix.

Table 1
Summary of literature review undertaken.

Reference	Staggered load restoration	Indoor temperature dynamics	TCL model description	Type of TCL	Limiting rebound effect at a component level
[8]	–	✓	✗	Heat pump	✗
[9]	–	✗	✗	✗	✗
[10]	–	✓	✗	Electric heating	✗
[11]	–	✗	✗	✗	✗
[12]	–	✓	✗	Air conditioner	✗
[13]	✓	✓	✗	✗	✗
[14]	✓	✗	✗	✗	✗
[15]	✓	✓	✗	Air conditioner	✗
[16]	✓	✗	✗	✗	✗
[17]	✓	✗	✗	✗	✗
[18]	✓	✗	✗	✗	✗
[19]	✓	✗	✗	✗	✗
[20]	✓	✗	✗	✗	✗

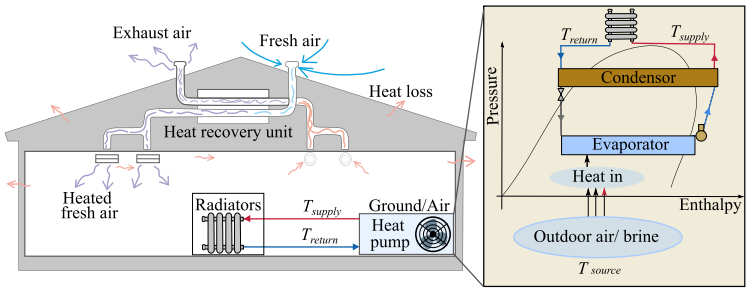

Fig. 1. Illustrative overview of various aspects considered in the thermal modelling of houses equipped with heat pumps.

2.3. An overview of the indoor temperature controller used in this study

As the dynamics of the indoor temperature is slow, a proportional–integral (PI) controller with an anti-wind-up and a feed-forward structure is selected for controlling the indoor temperature. A possibility could have been to instead use a proportional–integral–derivative controller (PID). However, due to the low sensitivity to disturbances that a PI controller has in relation to a PID controller, a PI controller is selected. The anti-wind-up structure ensures that there is no overshoot in the indoor temperature due to the integration of the difference between the reference and the actual indoor temperature during the problematic period in the integral controller.

The general flow chart of the indoor temperature controller is shown in Fig. 2. The key feature of the proposed model lies in the delivery of maximum heat during the recovery period without using electric heating. This concept is explained in the next section.

2.4. Concept behind the proposed heat pump controller

The proposed controller design in this article is based on accounting for the maximum heat delivering capability of the heat pump and the installed radiators in the house.

The characteristics of the heat-delivering capability of a heat pump with possible Coefficient of performance (COP) values are shown in Fig. 3. It is observed that, as the radiator water supply temperature 'T_{supply}' increases, the heat delivering capability and the COP reduces accordingly.

The characteristics of the heat delivering capability of the radiators based on 'T_{supply}' and 'T_{room}' are also shown. It is observed that as 'T_{supply}' increases, the heat-delivering capability of the radiators also increases.

The maximum heat delivering capability of the heat pump is indicated by the red line. It is interesting to note that even though the radiators have a high heat delivering capability at higher water supply temperatures, the heat delivered will be limited by the maximum heat delivering capability of the heat pump, if the electric heating is disabled.

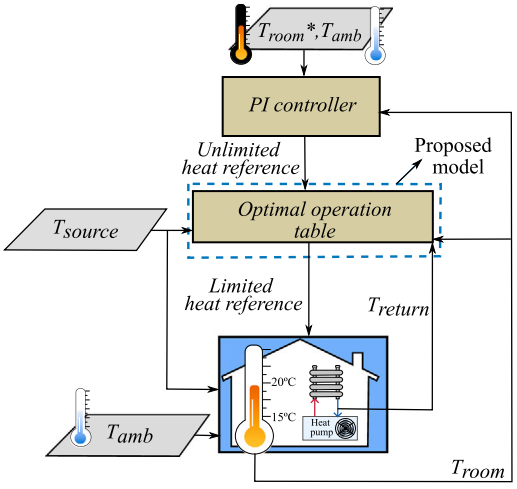

Fig. 2. General flow chart of the indoor temperature controller.

The desired heat is represented using a maroon circle and the heat attained using the standard and proposed controller are represented with a pink diamond and a green circle, respectively.

As the desired heat is typically higher during the recovery period, the standard controller chooses a higher value of the supply temperature to deliver a high heat. However, because of the lack of information regarding the heat delivering capability of the heat pump, a lower heat is obtained instead.

The proposed controller can, by accounting for the maximum heat delivering capability of the heat pump and the radiators, provide the estimates of water supply temperatures to deliver maximum heat at various indoor temperatures. This is highlighted using the green box in Fig. 3. Thus, the heat delivered by the heat pump using the standard controller will be lower, compared to using the proposed controller with electric heating disabled.

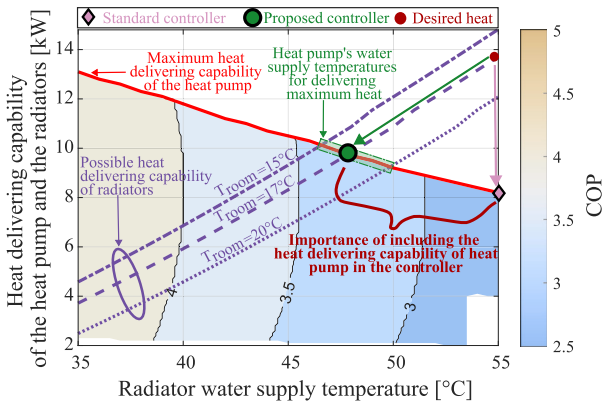

Fig. 3. Concept of the proposed heat pump controller.

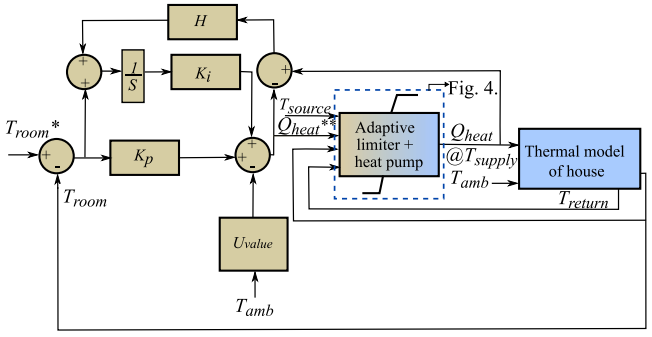

Fig. 4. Indoor temperature controller.

This result becomes very important during the recovery period where maximum heat is required to restore the indoor temperature to the pre-disturbance condition as fast as possible, while ensuring a high COP during the whole process.

2.5. Indoor temperature controller

The schematic representation of the indoor temperature controller to reduce the rebound effect of using flexibility is shown in Fig. 4.

Here K_p, K_i and H represent the proportional, integral, and anti-wind up gains, respectively. The controller is based on the internal model control principle [23]. Here, the control parameters are expressed in terms of the estimates of the thermal resistance and thermal capacitance of the house followed by the desired bandwidth of the controller.

The adaptive limiter flow chart is shown in Fig. 5. The main feature of this limiter is to obtain the estimate of the water supply temperature provided by the heat pump to deliver maximum heat at a given indoor temperature.

The radiator look-up table (LUT) is formulated based on the radiator model presented in Appendix, referring to [21]. This table is formulated for a given temperature difference ΔT between $\hat{T}_{supply}*$ and $\hat{T}_{return}*$ in the radiators. The characteristics of the radiator LUT can be seen in Fig. 3, represented by purple curves. Based on $Q_{heat}{}^{**}$, T_{room}, the radiator LUT provides $\hat{T}_{supply,rad}*$. This is an advanced version of a standard weather-compensated heat pump control, where the selection of supply temperature based on the desired heat and the actual room temperature is automated.

Similarly, based on the values of T_{room} and T_{source}, the heat pump supply temperature LUT provides $\hat{T}_{supply,maxheat}*$, calculated to deliver maximum heat through radiators at a given indoor temperature, without using electric heating. The characteristics of this LUT resemble

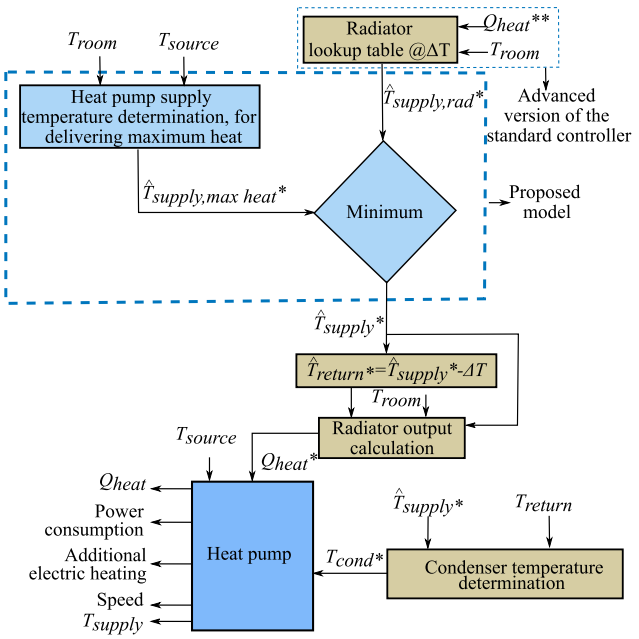

Fig. 5. Flow chart of the adaptive limiter.

the area highlighted in the green box in Fig. 3. This is a very critical feature that needs to be adhered to; otherwise, the rebound effect will be both power and energy intensive. The procedure for determining this is explained in Appendix. $\hat{T}_{supply,rad}*$ and $\hat{T}_{supply,max\ heat}*$ are compared and the lowest value is chosen.

Now, the estimates of $\hat{T}_{supply}*$ and $\hat{T}_{return}*$ can be determined. Using the above information and by using T_{room}, the reference value $Q_{heat}{}^{*}$ considering the limitations in the radiators is determined using the radiator model. Furthermore, $T_{cond}{}^{*}$ is calculated using $\hat{T}_{supply}*$ and T_{return} as indicated in Appendix [24].

Finally, the heat pump model using the values of $T_{cond}{}^{*}$, $Q_{heat}{}^{*}$ and T_{source} provides the values of Q_{heat}, the total electric power consumption by the heat pump, the compressor speed and T_{supply}.

The purpose of the procedure presented in this section is to ensure that during the recovery period, COP stays as high as possible.

2.6. Maximum rebound electric power

The maximum rebound electric power '$P_{rebound}$' during indoor temperature recovery is estimated as

$$P_{rebound} = max\,(P(t)), \quad t \in recoveryperiod \tag{1}$$

Here 'P' refers to electric power consumption.

The reduction in peak electric power consumption achieved by the proposed controller $P_{rebound,proposedcontroller}$ compared to the standard controller $P_{rebound,standardcontroller}$ is determined as

$$\frac{P_{rebound,\ standard\ controller} - P_{rebound,\ proposed\ controller}}{P_{rebound,\ standard\ controller}} \tag{2}$$

3. Case study

Taking Sweden as an example, the geographical limit for this study is chosen to be the southern half, as the electricity demand in this region is much higher compared to the northern half.

An outdoor ambient temperature of −5 °C is considered for the analysis representing a medium cold day during winter. Based on Ref. [25], the indoor temperature is set to be 20 °C during normal operating conditions.

Table 2
Parameters considered for thermal modelling of houses [4].

House type	Year of construction	U_{value} $\left(\frac{W}{m^2\ K}\right)$	Time constant (h)	Infiltration $\left(\frac{l}{s\ m^2}\right)$	η of heat recovery	Heat emitter	Type of heat pump	Number of radiators	Number of houses
1	1961–1975	1.06	34	0.80	0.00	Radiators	Ground source	14	445 500
2	1976–1985	0.82	40	0.80	0.60	Radiators	Air to water	15	274 322
3	1986–1995	0.72	53	0.80	0.60	Radiators	Air to water	12	147 400

A power deficit event now occurs at hour 6.75 and the heat pumps in this scenario are programmed to provide support for the power system, and as a consequence the indoor temperature will be set to be lowered from 20 °C to 18 °C and 15 °C respectively, if the disruption will be long-term. The former case represents a moderate demand response case and the latter represents a serious situation with a severe power deficit condition.

3.1. Input data for heat pump modelling

The air-to-water and ground-to-water heat pumps are assumed to be equipped with a ZPV030 Copeland–Emerson scroll compressor and the maximum compressor rating is 3 kW. The maximum rating of the additional electric heating is set at 3 kW.

Based on the data available in [26,27], a temperature drop of 10 °C and 8 °C, between 'T_{source}' and the evaporator temperature, is used for the ground source and the air source heat pumps respectively.

T_{source} for the ground source heat pump and air source heat pump is assumed to be the ground (10 °C) and the outdoor ambient temperature, respectively.

3.2. Input data considered thermal modelling of houses

The thermal and physical properties of the houses equipped with heat pumps considered for the analysis are shown in Table 2, originally from [4,28]. The time constants used are based on the range of values stated in [29,30], and on the analysis of the result presented in [4]. The average size of Swedish single family houses is 122 m^2 [31] and this value is used in the analysis.

A ventilation rate of 0.35 $\left(\frac{l}{s\ m^2}\right)$ is used for all houses. The houses constructed before 1961 are excluded from the analysis, encompassing a conservative approach.

Purmo radiators of type PURMO C 33 400 × 1000 [32] are considered for the analysis. A ΔT of 10 °C is chosen for the analysis based on [33,34].

4. Results and discussion

House type 1, which is a typical house constructed during 1961–1975 is taken as an example to present an in-depth analysis on a component level, as they are high in number compared to other house categories.

The target indoor room temperature recovery from 15 °C to 20 °C, after providing flexibility through reducing the indoor temperature from 20 °C to 15 °C over a period of 17.25 h, is chosen to represent an extreme situation with a severe power deficit condition in this article. Similarly, a target recovery of indoor room temperature from 18 °C to 20 °C, after providing flexibility by reducing indoor temperature from 20 °C to 18 °C over a period of 3.25 h, is chosen to represent a mild demand response condition.

Furthermore, the case with the standard heat pump controller refers to an advanced version of the standard weather-compensated heat pump control where T_{supply} is changed to meet different heating requirements. This standard controller does not include the estimation of the water supply temperature to provide maximum space heating through radiators, considering the limitations of heat pumps. However, this is included in our proposed controller. MATLAB is used for the numerical simulations.

Table 3
Comparison of result obtained with data provided in [35].

Compressor model	ZPV030	
	Given	Obtained
Speed (RPM)	3600	3600
Rated capacity (kW) @ ARI 3600 RPM	9.7	10.35
Electric power input (kW)	2.98	2.94
COP (W/W)	3.25	3.52

4.1. Heat pump

The heat pump model is validated by comparing the results obtained under standard air conditioning and refrigeration institute conditions, i.e., 7.2 °C evaporator temperature, 54.4 °C condenser temperature, with super heating of 11 °C and sub-cooling of 8.3 °C, with the data given in [35].

The results are tabulated in Table 3 and the agreement is good. A discrepancy of 6.7% is observed in the heat delivered. This might be because heat losses in the evaporator are not taken into account. However, the results of the electric power consumption from the model presented agree well with the data provided in [35].

4.2. Recovery analysis using the proposed heat pump controller, during an extreme situation

Fig. 6 shows the thermodynamics in the house before supporting the power system, then while supporting by reducing the electric power drawn, and finally during recovery of the indoor temperature to pre-disturbance conditions. The results obtained from the proposed controller are presented in bright colours, whereas those from the standard controller are represented in dark colours. The corresponding selected operating points are represented using green circles and pink diamonds, respectively.

The mapping of the selected operating points, considering the heat delivering capabilities of the heat pump and the installed radiators for the proposed and standard controller, are shown in Fig. 7. Here, the desired heat value is represented using maroon circles.

In this study, the objective is to obtain the same recovery time for both the standard and the proposed controller, but with the proposed controller managing this without the electric heater.

It is observed that before providing support, the indoor temperature is maintained at 20 °C. During the support time, the reference value of the indoor temperature is reduced to 15 °C. As desired, there is a period without heat and electric power consumption when the indoor temperature is reduced. The power system has now been relieved of 2.1 kW for some time. This is followed by a period with reduced heat and electric power consumption as the corresponding requirements are lower to maintain the indoor temperature at 15 °C compared to maintaining it at 20 °C. This can be seen in Figs. 6(a)–6(c). The corresponding COP, water supply and return temperature in the radiators, followed by the speed of the heat pump, is shown in Figs. 6(d)–6(f), respectively. During this period, in Figs. 6 and 7 it is observed that the actual and desired heat are the same using both the proposed and the standard controller.

During the recovery period, the reference value of the indoor temperature is ramped up starting at hour 24 to restore the indoor temperature by hour 30. From Figs. 6 and 7, during the recovery period,

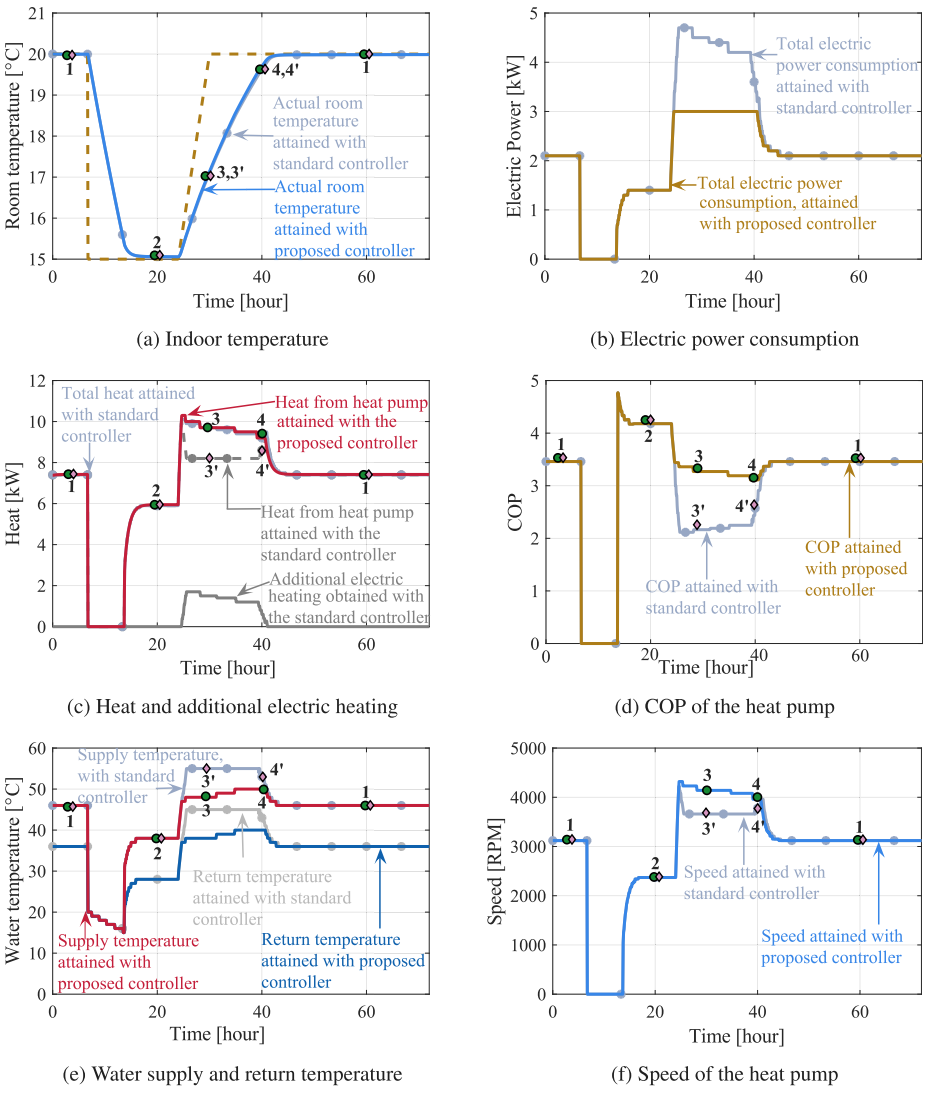

(a) Indoor temperature

(b) Electric power consumption

(c) Heat and additional electric heating

(d) COP of the heat pump

(e) Water supply and return temperature

(f) Speed of the heat pump

Fig. 6. Comparison of recovery analysis after providing flexibility during severe power deficit conditions, with the standard and the proposed controller, in house type 1.

it is seen that there is a change in the operating points both when using the proposed and standard controller. Higher values of supply temperatures are chosen to deliver a high value of heat using the standard controller compared to the proposed controller. However, due to limitations in the heat delivering capability of the heat pump at these supply temperatures, additional electric heating is utilised to deliver the same heat as in the case of the proposed controller, which, of course, is strongly undesirable. The result is that, the COP is higher and the electric power consumption is lower using the proposed controller compared to the standard controller.

It does not help to have the electric heating blocked in the standard controller, as the indoor temperature recovery will now take a longer time due to limitations in the heat delivering capability of the heat pump at high supply temperatures and accordingly, the duration with 3 kW peak power consumption will be longer compared to our proposed controller.

The electric power consumption in house types 2 and 3 is shown in Figs. 8(a) and 8(b), respectively. The evolution of indoor temperatures in these houses is shown in Fig. 8(c). In Table 2 it is observed that the thermal inertia in the above houses is high and therefore recovery takes a longer time compared to house type 1. As house type 3 has the highest thermal inertia, indoor temperature recovery has a longer duration compared to the two previous types of house. It should be mentioned that during the flexibility period, the duration without electric power consumption increases with an increase in the thermal inertia of the house as witnessed in Figs. 8 and 6(b). Furthermore, as indoor temperatures reach the target value of 20 °C, the electric power consumption is reduced accordingly and eventually reaches a steady state value.

This prepared resilience action from a number of buildings has the potential to save the power system from a disastrous event, where a black-out would be the alternative. Thus, it is unavoidable that general regulations regarding indoor climates are violated. The indoor temperature stays below 18 °C for a duration of 23 h, 25 h, 25.9 h in house types 1,2 and 3, respectively. Houses that provide flexibility by compromising thermal comfort should thus be compensated accordingly.

From Figs. 8 and 6(b), it is observed that with the proposed controller, in house types 1, 2 and 3, the peak power consumption is 1.7 kW and 1.3 kW lower, respectively, compared to the standard controller. Thus, achieving a reduction in rebound power consumption by about 36% and 30%, respectively. This clearly signifies the importance of matching the maximum heat delivering capability of the heat pump with the installed radiators, using the proposed controller.

Furthermore, it is observed that the performance in both the controllers matches exactly during pre-disturbance and flexibility periods,

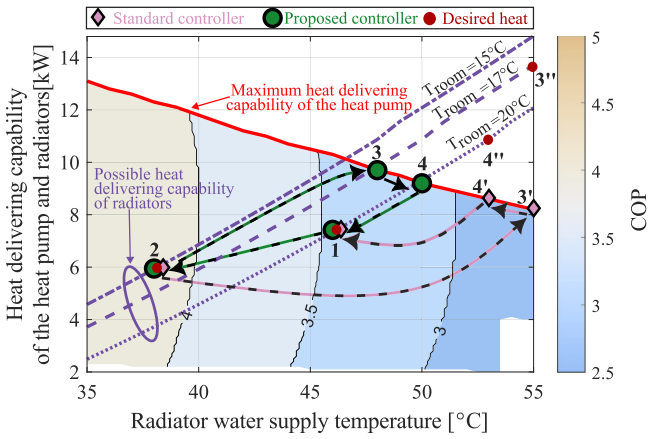

Fig. 7. Operating points obtained using standard and the proposed controller, in house type 1.

clearly emphasising the strength of the proposed controller during recovery periods.

4.3. Sensitivity analysis

4.3.1. Variations in radiator number and infiltration rate

A sensitivity analysis is performed to test the performance of the proposed controller compared to the standard controller, considering a variation in the number of radiators and the infiltration rate.

As mentioned earlier, the objective of this study is to obtain the same recovery time for both the standard and the proposed controller, and, in addition, with the proposed controller managing this without the electric heater.

The time taken to recover indoor temperatures considering a variation of ±15% in the number of radiators and ±10% variation in infiltration rates, compared to the values in Table 2 is shown in Fig. 9. The corresponding reduction in peak electric power consumption using the proposed controller compared to the standard controller is shown in Fig. 10.

With a reduced number of radiators, higher supply temperatures are required to deliver the same heat as in the case with a high number of radiators. The heat delivering capacity of heat pumps at high supply temperatures is reduced as seen in Fig. 7. Thus, as the heat capacity is limited at higher water supply temperatures, the recovery time increases. However, with a higher number of radiators, the recovery time is reduced because the heating capacity of the heat pumps is relatively higher at lower supply temperatures compared to the former case. This is observed in Fig. 9.

Infiltration rates correspond to heat losses in houses. Thus, the lower the infiltration rate, the shorter the recovery time.

In Fig. 10 it is observed that as the number of radiators increases, the reduction in peak electric power consumption compared to the standard controller increases. This is because the heat delivering capability of the radiators at lower supply temperature increases with an increase in the number of radiators. This means that the maximum heat that can be provided during the recovery period using the proposed controller also increases. As the standard controller chooses a higher supply temperature where the heat pump's heating capability is limited, additional electric heating needed to deliver the same heat as in the case of the proposed controller increases.

The sensitivity analysis undertaken further demonstrates the strength of the proposed controller compared to the standard controller in reducing peak electric power consumption.

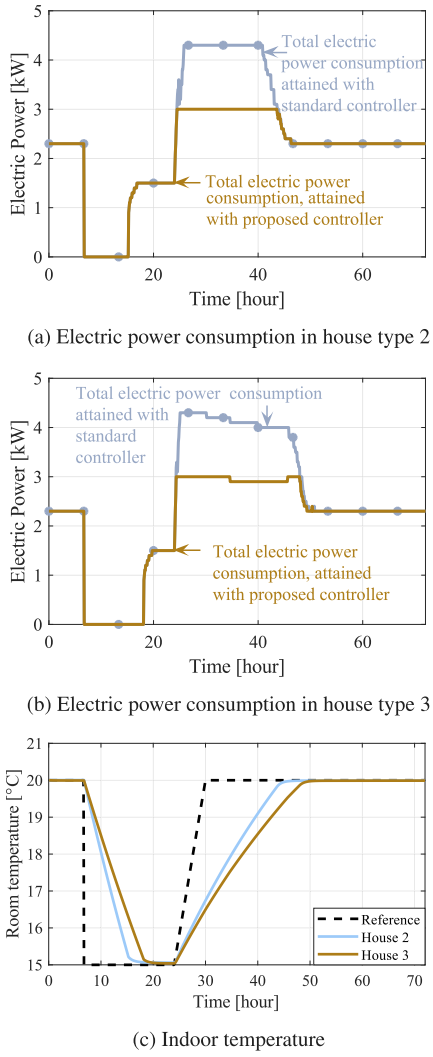

Fig. 8. Indoor temperature and comparison of electric power consumption between the standard and the proposed controller after providing flexibility during severe power deficit conditions, in house types 2 and 3.

4.3.2. Variations in the difference between the supply and return water temperature in radiators

Sensitivity analysis considering the variation in the difference between 'T_{supply}' and 'T_{return}' in the radiators is performed to test the performance of the proposed controller. Based on Refs. [33,34], the difference between 'T_{supply}' and 'T_{return}' vary between 5 °C and 10 °C for space heating systems equipped with heat pumps. Hence, the same is considered for the sensitivity analysis. The other details of three house types are described in Table 2. The results of this sensitivity analysis is shown in Fig. 11.

In Fig. 11, it is observed that the influence of the difference between 'T_{supply}' and 'T_{return}' in the radiators on the performance of the proposed controller is not significant.

4.4. Recovery analysis using the proposed heat pump controller, during a moderate disturbance situation

Fig. 12 shows the consumption of electric power in the houses under study, while providing a moderate demand response by reducing the indoor temperature from 20 °C to 18 °C over a period of 3.25 h. In this case, the thought is that we perhaps only perform energy arbitrage. The analysis also includes the target indoor temperature recovery to 20 °C

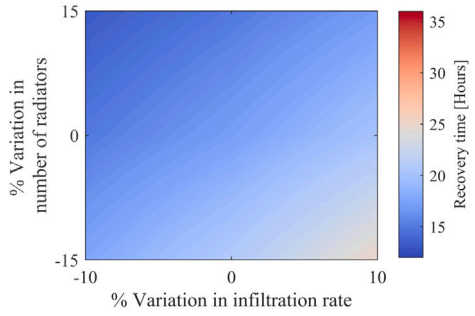

(a) Indoor temperature recovery time in house type 1

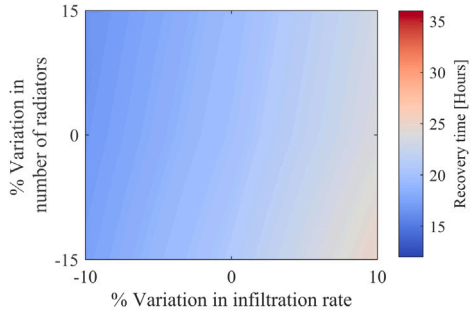

(b) Indoor temperature recovery time in house type 2

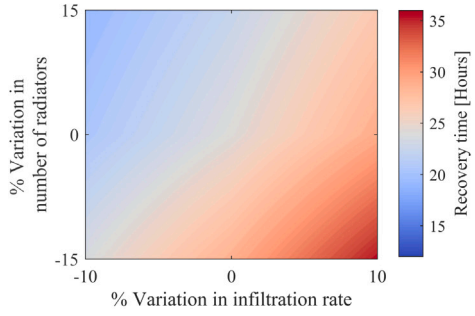

(c) Indoor temperature recovery time in house type 3

Fig. 9. Sensitivity analysis of variation in the number of radiators and infiltration rate on indoor temperature recovery time.

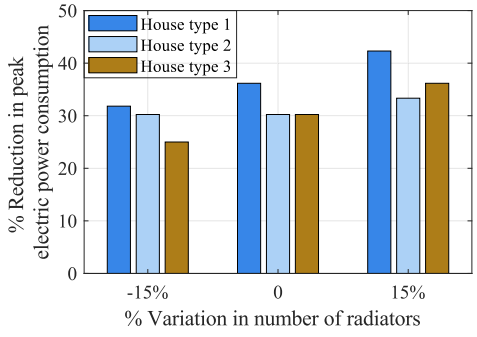

Fig. 10. Sensitivity analysis of variation in the number of radiators on the reduction in peak electric power consumption during recovery period, using the proposed controller compared to the standard controller.

in two hours, while ensuring a high COP. The results obtained with the proposed controller and the standard controller are represented in bright and dark colours, respectively. Here also, the objective is to ensure indoor temperature recovery at the same time using both controllers, and electric heating is disabled in the case of the proposed controller.

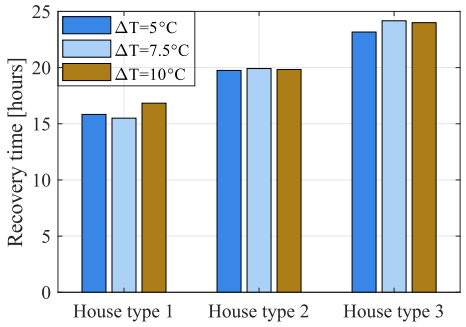

Fig. 11. Sensitivity analysis on the recovery time considering variations in the difference between the supply and return water temperature in radiators, using the proposed controller.

As witnessed previously, due to limitations in the heat pump's heat delivering capability at higher values of supply temperatures, additional electric heating is needed in the case of the standard controller to deliver the same heat as in the case of the proposed controller. Thus, using the proposed controller, the rebound power is substantially lower. The key feature is that the proposed controller manages to have a higher COP compared to the standard controller.

Figs. 12(a)–12(c) reveal that during the recovery period, a reduction in peak electric power consumption by 31%, 30% and 29% is achieved in house types 1, 2, and 3, respectively, using the proposed controller compared to the standard controller. This clearly highlights the significance of the proposed controller in limiting the rebound effect of using heat pumps after participating in moderate demand response programmes.

4.5. Quantification of electric power consumption as a function of time by heat pumps providing flexibility, including recovery on a system level

The quantification of the electric power consumption by heat pumps on a system level, during the flexibility and recovery periods is based on the following assumptions

- The initial indoor temperatures in all the houses under study is assumed to 20 °C.
- The signals for indoor temperature set points during flexibility and recovery periods in all the houses under study are synchronised.

A great advantage with variable speed pumps is that synchronised turn-on has a much smaller impact compared to fixed-speed pumps. In addition, when utilising this resource, of course a safety band must be utilised, and that is the reason why only 44% of the total single family buildings' capacity has been utilised.

4.5.1. Recovery analysis during extreme situations

The quantification of electric power consumption as a function of time by 0.87 million heat pump equipped houses is shown in Fig. 13. The details of these houses are indicated in Table 2 and the quantification is based on the results presented in Section 4.2 during extreme situations.

It is observed that about 1.9 GW of electric power is required to maintain indoor temperatures at 20 °C in 0.87 million houses. Consequently, the power system can be relieved of 1.9 GW, and in our example, this reduction is for 7 h and then 650 MW for the next 10 h, with the consequence of the indoor temperatures dropping to 15 °C.

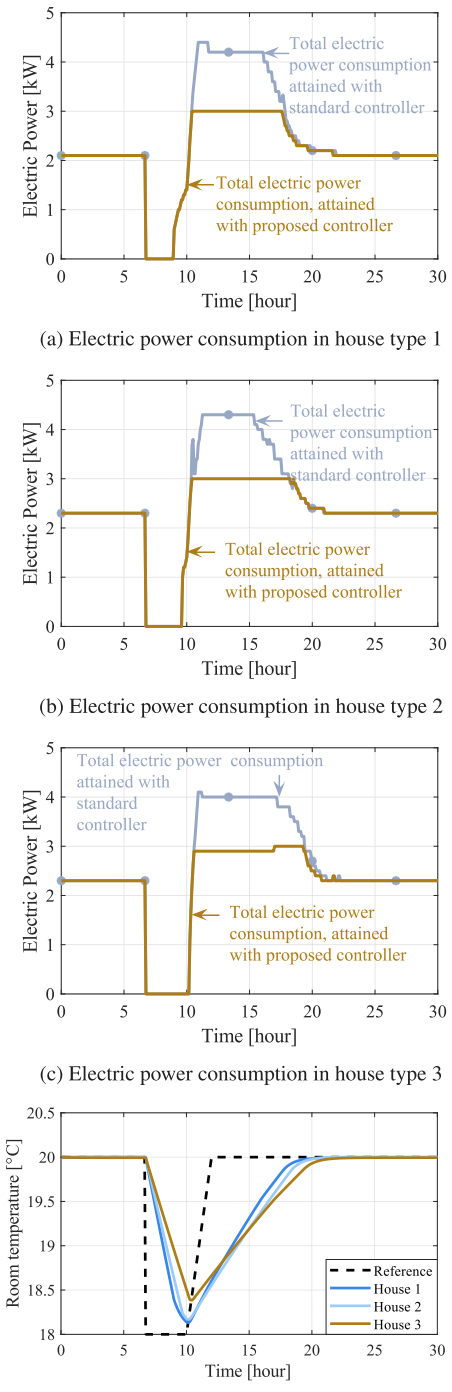

Fig. 12. Indoor temperature and comparison of electric power consumption between the standard and the proposed controller after providing flexibility during mild demand response program, in house types 1, 2 and 3.

During indoor temperature recovery to 20 °C taking 20 h, using the proposed controller, the maximum rebound power is limited to 2.6 GW compared to 3.9 GW using the standard controller. Thus, achieving a 33% reduction in peak power consumption.

This shows that the proposed controller helps to limit the CLPU effect by reducing the peak power consumption of the heat pumps after providing flexibility during extreme situations. These results help system operators during recovery periods, in taking informed decisions

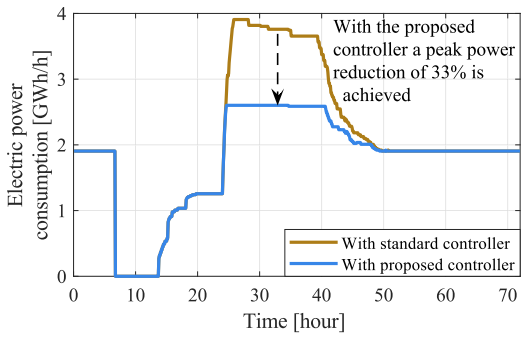

Fig. 13. Quantification of electric power consumption by heat pumps prior to providing support to the power system, while supporting by reducing the indoor temperature from 20 °C to 15 °C and during recovering the indoor temperature to 20 °C, using the standard and the proposed controller.

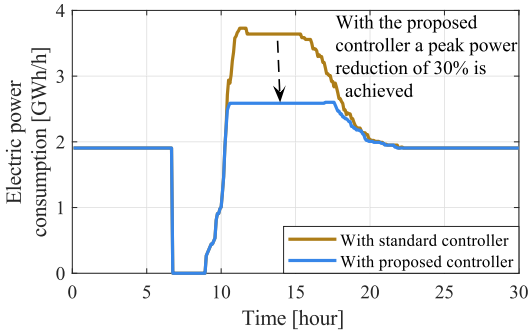

Fig. 14. Quantification of electric power consumption by heat pumps prior to providing support to the power system, while supporting by reducing the indoor temperature from 20 °C to 18 °C and during recovering the indoor temperature to 20 °C, using the standard and the proposed controller.

in load management while balancing power systems with limited generation and importing capacity, which is a key feature in increasing grid resilience.

4.5.2. *Recovery analysis during moderate disturbance situations*

The quantification of electric power consumption as a function of time by 0.87 million heat pumps in the study, based on the results presented in Section 4.4 during moderate disturbance situations, is shown in Fig. 14.

Here also the analysis remains the same as in the case of Fig. 13, where the power grid is relieved of 1.9 GW for about 2 h. During the recovery period, a peak power reduction by 30% is obtained using the proposed controller compared to the standard controller. This emphasises the proposed controller's strength in limiting the CLPU effect occurring also after providing flexibility during moderate problematic situations.

4.6. *Future work*

There are many further investigations needed, some proposed valuable efforts are

- Experimental validation of the proposed controller in a heating system equipped with a heat pump.
- Quantification of the rebound electric power consumption in a system with both space and water heating equipped with a heat pump, accounting for the withdrawal of hot water from the occupants during the recovery period.

- Employing stochastic models to quantify flexibility and rebound effect in 0.87 million houses, to account for the uncertainty in the buildings thermal properties such as heat transfer coefficient, infiltration, number of radiators, and indoor temperature set points based on the occupants behaviour.

4.6.1. Practical deployment of the controller

In a practical employment of this support functionality, it would be needed to know the maximum heating capability of the heat pump, heat delivering capabilities of the radiators, and U_{value} of the house.

Some heat pump manufacturers, such as NIBE, are helping customers reduce their electricity bill by remotely steering heat pumps based on electricity prices. In this case, the information regarding the heating capability of the heat pump at various source temperatures is known beforehand. The U_{value} can also be obtained later, using the outdoor and indoor temperature sensor data and the heat metres incorporated in the heat pump units. Finally, radiator data can be accessed from standard radiator types. So, proposed controller can be implemented and incorporated in the heat pump by heat pump manufacturers. Even if heat pumps are controlled by other aggregators, by making set point changes in the indoor temperature, the heat pump units would autonomously avoid undesirable overshoot during the recovery period.

5. Conclusion

The rebound effect of using flexibility of space heating systems equipped with heat pumps can have large negative CLPU effects, while restoring the indoor temperature to normal conditions. Furthermore, the fact that the participation of heat pumps in dynamic pricing schemes leads to substantial CLPU effects is confirmed in [6].

Today, modern variable speed heat pumps are dominating new installations strongly, and they will soon dominate the accumulated installations. Thus, in this article, the possibility to limit the CLPU effects on a component level considering variable speed heat pumps is investigated i.e. a deeper analysis of the electric power consumption by heat pumps with the associated thermal effects is undertaken on a component level, which so far has been missing in scientific literature.

An adaptive heat pump controller is proposed to provide maximum possible space heating during the recovery period, considering the limitations in heat pumps. The peak electric power required is much lower using the proposed controller compared to the standard heat pump controller, while recovering the indoor temperature at the same time. This shows that the proposed controller helps to limit the CLPU effects by reducing the peak electric power consumption of the heat pumps during the recovery period.

Taking the southern half of Sweden as an example, at −5 °C outside temperature, approximately 1.9 GW dedicated for heating is required to maintain indoor temperatures at 20 °C, in 44% of single-family houses. The power system can be relieved of these 1.9 GW for 7 h and 650 MW during 10 h, with the consequence that the indoor temperatures drop to 15 °C. During an indoor temperature recovery to 20 °C, over 20 h using the proposed controller, the maximum rebound power is limited to 2.6 GW compared to 3.9 GW using the standard controller. Thus, achieving a 33% reduction in peak power.

During the same conditions, indoor temperatures are reduced from 20 °C to 18 °C over a duration of 3.25 h, to represent a moderate demand response case. A target temperature recovery to 20 °C is achieved in 10 h and the recovery peak power is limited to 2.6 GW as opposed to 3.7 GW, which is about a 30% reduction compared to the standard controller. Thus, with the proposed controller, the CLPU effects are limited, thereby reducing the rebound effect during the recovery period, after participating in moderate demand response programmes.

In this article, the effectiveness of the proposed controller is clearly demonstrated. The proposed controller aids in limiting rebound effects of using flexibility from heat pumps, after supporting the power systems during moderate situations and also during extreme events with severe power deficit conditions.

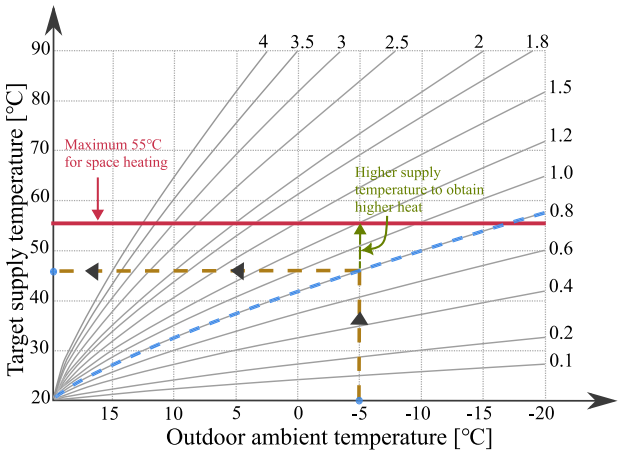

Fig. 15. An example heating curve [36].

CRediT authorship contribution statement

Sindhu Kanya Nalini Ramakrishna: Writing – review & editing, Writing – original draft, Visualization, Validation, Methodology, Investigation, Formal analysis, Data curation, Conceptualization. **Torbjörn Thiringer:** Writing – review & editing, Supervision, Software, Resources, Project administration, Methodology, Conceptualization. **Peiyuan Chen:** Writing – review & editing, Supervision.

Declaration of competing interest

The authors declare that they have no known competing financial interests or personal relationships that could have appeared to influence the work reported in this paper.

Acknowledgement

The financial support provided by the Swedish Energy Agency, Sweden through Grant No. 50343-1 is gratefully acknowledged.

Appendix

A.0.1 Standard weather compensated heat pump controller

The weather-compensated heat pump controller is based on the heating curves. An example heating curve is shown in Fig. 15 [36]. This provides information on the different water supply temperatures required in houses to meet the space heating requirements at different outdoor ambient temperatures.

Based on the heating requirements of a house, a specific heating curve is selected. For example, in Fig. 15, if the heating curve of 0.8 is selected, which is indicated by the blue dashed line, this curve will be used as a reference to obtain the required supply temperatures at different outdoor ambient temperatures. For example, at an outdoor ambient temperature of −5 °C, a supply temperature of about 46 °C is maintained. If additional heating is required, the heating curve is shifted up, where a higher supply temperature is selected to deliver a higher heat. This is indicated by the green arrow. Typically for heat pump systems with radiators in Sweden, the maximum supply temperature in the radiators is limited to 55 °C and this is indicated by the solid red line.

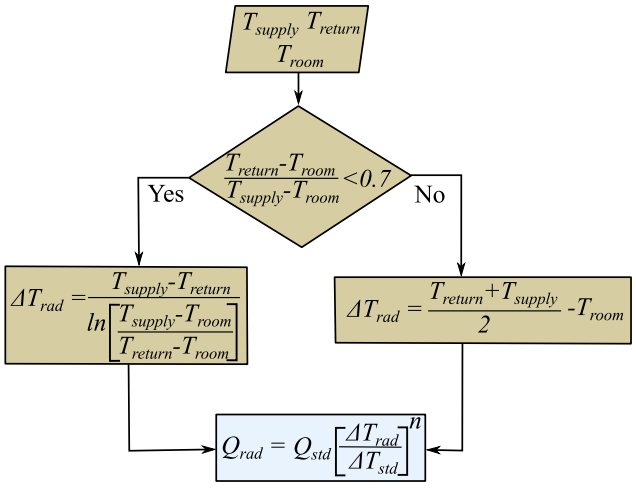

Fig. 16. Radiator model [21].

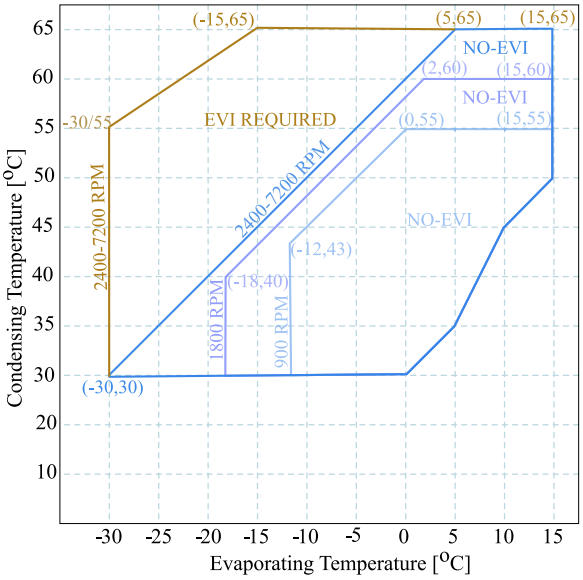

Fig. 17. Operating envelope considered for study [35].

A.0.2 Modelling of radiators

The thermal output of the radiators is modelled as shown in Fig. 16 [21,32]. Q_{std} and ΔT_{std} represent the total heat output from radiators and reference temperature at standard conditions (i.e., at 55 °C supply temperature, 45 °C return temperature and 20 °C room temperature) respectively. The term n refers to the exponent characteristic of the radiator.

A.0.3 Calculation of condenser temperature

The condenser temperature $T_{cond}{}^{*}$ in the heat pump, based on the supply and return temperature of the water [37] can be calculated as

$$T_{cond}{}^{*} = T_{return} + \frac{\hat{T}_{supply}{}^{*} - T_{return}}{1 - e^{\frac{-(\hat{T}_{supply}{}^{*} - T_{return})}{\Delta T_{log.cond}}}} \tag{3}$$

A.0.4 Operating envelope of the heat pump

The operating envelope indicates the operating points within which the heat pump can operate safely and the performance is guaranteed. The operating envelope considered for this study is shown in Fig. 17.

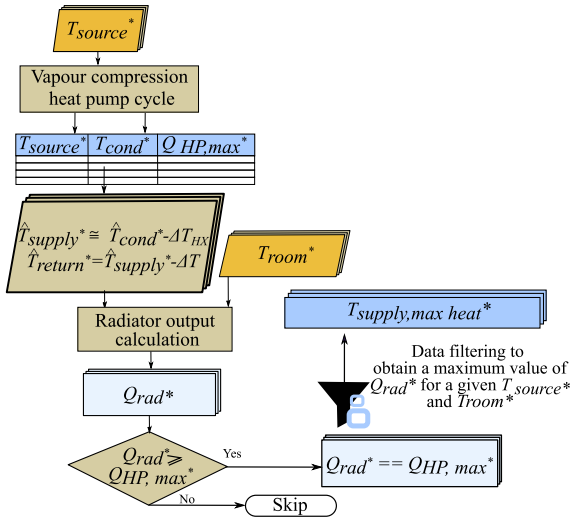

Fig. 18. Flow chart for creating LUT to estimate heat pump's water supply temperature for delivering maximum heat via radiators.

A.0.5 Algorithm for estimating heat pump's supply temperature for delivering maximum heat via radiators

The algorithm for estimating the supply temperature of the heat pump to deliver maximum heat via the radiators is shown in Fig. 18. This algorithm is proposed because the heat delivery capability of the heat pump is reduced with an increase in the water supply temperature, as seen in Fig. 3. This is the key feature of the proposed control structure.

The maximum value of heat delivered by the heat pump $Q_{HP,max}{}^{*}$ corresponding to various values of $T_{source}{}^{*}$ and $T_{cond}{}^{*}$ is obtained using the vapour compression heat pump cycle.

Based on the data available in [33] [34], the temperature difference between $\hat{T}_{supply}{}^{*}$ and $\hat{T}_{return}{}^{*}$ vary between 5 °C and 10 °C. Furthermore, by analysing the desired $T_{cond}{}^{*}$ for various values of $T_{supply}{}^{*}$ and $T_{return}{}^{*}$ using (3) [24], a temperature difference of 1 °C–2 °C is found between $T_{cond}{}^{*}$ and $T_{supply}{}^{*}$. The difference between $T_{cond}{}^{*}$ and $T_{supply}{}^{*}$ is represented as ΔT_{HX}.

For different room temperature values in combination with various values of $\hat{T}_{supply}{}^{*}$ and $\hat{T}_{return}{}^{*}$ at a given ΔT, the heat delivered by the radiators $Q_{rad}{}^{*}$ is calculated using the radiator model.

This is followed by checking in each case if $Q_{rad}{}^{*}$ is greater than $Q_{HP,max}{}^{*}$. In that case, the heat emitted by the radiators is made equal to $Q_{HP,max}{}^{*}$. Finally, the values obtained for various cases are tabulated. This is followed by data filtering to obtain the maximum value of $Q_{rad}{}^{*}$ with the corresponding $\hat{T}_{supply}{}^{*}$ obtained for a given combination of $T_{source}{}^{*}$ and $T_{room}{}^{*}$. Thus, $\hat{T}_{supply,max\ heat}{}^{*}$ is obtained for a given combination of $T_{source}{}^{*}$ and $T_{room}{}^{*}$.

A.0.6 Indoor temperature controller analysis

As the controller in this article is based on internal model control principle [23], the proportional and integral gains depend on the estimates of the thermal parameters of the house (thermal capacitance and thermal resistance) as well as the desired bandwidth of the controller. Thus, to study the impact of uncertainty in estimates of houses' thermal parameters on the controller performance, a closed loop pole map considering variation in the thermal resistance $\hat{R}_{value}$ (R_{value} is the reciprocal of U_{value}. $\hat{R}_{value}$ is the estimated value set in the controller gains) for houses under study is shown in Fig. 19.

In Fig. 19, it is observed that all poles lie in the left half of the s-plane. The corresponding gain margins are infinite and the phase margins are ≥88° in all cases. Thus, the stability of the indoor temperature controller is ensured.

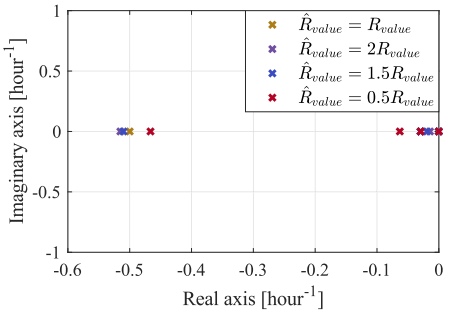

(a) House type 1

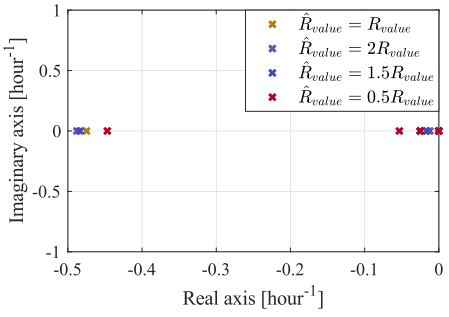

(b) House type 2

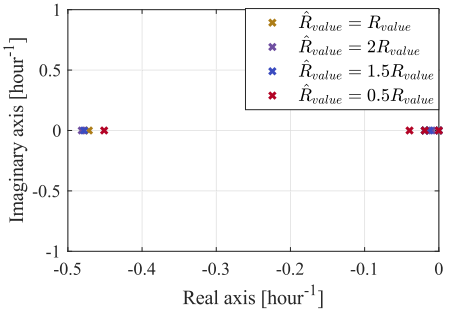

(c) House type 3

Fig. 19. The closed loop pole map of the indoor temperature control system in Fig. 4 for the three types of houses.

A.0.7 Details of the proposed indoor temperature controller

Using the internal model control principle [23], the overall transfer function of the indoor temperature control system in Fig. 4 is designed as a low pass filter. The proportional (K_p), integral (K_i) and anti wind-up gains (H) of the controller are obtained as

$$\begin{aligned} K_p &= \alpha_c \hat{C}_{value} \\ K_i &= \alpha_c \left(\frac{1}{\hat{R}_{value}} \right) \\ H &= \left(\frac{1}{K_p} \right) \end{aligned} \tag{4}$$

Here, α_c, $\hat{R}_{value}$ and $\hat{C}_{value}$ correspond to the controller bandwidth followed by the estimates of the thermal resistance and thermal capacitance of the plant model (House), respectively.

As the entire system in Fig. 4 is designed as a low pass filter, the closed loop poles lie in the left half of the s-plane, ensuring the stability of the system. This is also witnessed in Fig. 19 for the three houses under study in this article.

Data availability

Data will be made available on request.

References

[1] Rajkumar VS, Ştefanov A, Presekal A, Palensky P, Torres JLR. Cyber attacks on power grids: Causes and propagation of cascading failures. IEEE Access 2023;11:103154–76.

[2] Saeed MH, Syed Kazmi H, Deconinck G. Bottom-up quantification of energy flexibility in cluster of residential heat pump systems. In: 2022 IEEE PES innovative smart grid technologies conference Europe. ISGT-Europe, 2022, p. 1–5.

[3] Plaum F, Ahmadiahangar R, Rosin A. Aggregated energy flexibility provision using residential heat pumps. In: 2022 IEEE 16th international conference on compatibility, power electronics, and power engineering. CPE-POWERENG, 2022, p. 1–5.

[4] Chen H, Ruud S, Markusson C. Energy flexibility using thermal mass for Swedish single-family houses. E3S Web Conf 2024;562:04003, [Online]. Available: https://doi.org/10.1051/e3sconf/202456204003.

[5] Plaum F, Rosin A, AhmadiAhangar R. Novel quantification method of aggregated energy flexibility based on power-duration curves. IEEE Access 2024;12:132825–37.

[6] McKenna K, Keane A. Residential load modeling of price-based demand response for network impact studies. IEEE Trans Smart Grid 2016;7(5):2285–94.

[7] Agneholm E. Cold Load Pick-up [PhD dissertation], Sweden: Chalmers University of Technology; 1999.

[8] Schneider KP, Sortomme E, Venkata SS, Miller MT, Ponder L. Evaluating the magnitude and duration of cold load pick-up on residential distribution using multi-state load models. IEEE Trans Power Syst 2016;31(5):3765–74.

[9] Bu F, Dehghanpour K, Wang Z, Yuan Y. A data-driven framework for assessing cold load pick-up demand in service restoration. IEEE Trans Power Syst 2019;34(6):4739–50.

[10] Lang WW, Anderson MD, Fannin DR. An analytical method for quantifying the electrical space heating component of a cold load pick up. IEEE Trans Power Appar Syst 1982;PAS-101(4):924–32.

[11] Benato R, Dambone Sessa S, Giannuzzi GM, Pisani C, Poli M, Sanniti F. A novel dynamic load modeling for power systems restoration: An experimental validation on active distribution networks. IEEE Access 2022;10:89861–75.

[12] Mortensen R, Haggerty K. Dynamics of heating and cooling loads: models, simulation, and actual utility data. IEEE Trans Power Syst 1990;5(1):243–9.

[13] Song M, nejad RR, Sun W. Robust distribution system load restoration with time-dependent cold load pickup. IEEE Trans Power Syst 2021;36(4):3204–15.

[14] Ucak C, Pahwa A. An analytical approach for step-by-step restoration of distribution systems following extended outages. IEEE Trans Power Deliv 1994;9(3):1717–23.

[15] Al-Nujaimi A, Abido MA, Al-Muhaini M. Distribution power system reliability assessment considering cold load pickup events. IEEE Trans Power Syst 2018;33(4):4197–206.

[16] Li YL, Sun W, Yin W, Lei S, Hou Y. Restoration strategy for active distribution systems considering endogenous uncertainty in cold load pickup. IEEE Trans Smart Grid 2022;13(4):2690–702.

[17] Wang Y, Su X, Song M, Jiang W, Shahidehpour M, Xu Q. Sequential load restoration with soft open points and time-dependent cold load pickup for resilient distribution systems. IEEE Trans Smart Grid 2023;14(5):3427–38.

[18] Wang M, Fan Z, Zhou J, Shi S. Research on urban load rapid recovery strategy based on improved weighted power flow entropy. IEEE Access 2021;9:10634–44.

[19] Menazzi M, Qin C, Srivastava AK. Enabling resiliency through outage management and data-driven real-time aggregated DERs. IEEE Trans Ind Appl 2023;59(5):5728–38.

[20] Qin C, Jia L, Bajagain S, Pannala S, Srivastava AK, Dubey A. An integrated situational awareness tool for resilience-driven restoration with sustainable energy resources. IEEE Trans Sustain Energy 2023;14(2):1099–111.

[21] Nalini Ramakrishna SK, Björner Brauer H, Thiringer T, Håkansson M. Social and technical potential of single family houses in increasing the resilience of the power grid during severe disturbances. Energy Convers Manage 2024;321:119077, [Online]. Available: https://www.sciencedirect.com/science/article/pii/S0196890424010185.

[22] Nalini Ramakrishna SK, Thiringer T. Modelling of heat pumps, controller for space and water heating. Technical report, Gothenburg: Chalmers University of Technology; 2024.

[23] Harnefors L. Control of variable-speed drives. Applied Signal Processing and Control, Department of Electronics, Mälardalen University; 2002.

[24] Nalini Ramakrishna SK, Thiringer T, Markusson C. Quantification of electrical load flexibility offered by an air to water heat pump equipped single-family residential building in Sweden. In: 14th IEA, heat pump conference. 2023.

[25] Blom N. Folkhälsomyndighetens allmänna rådom temperatur inomhus. 2014.

[26] Emerson climate technologies. Copeland scroll heating, heat pump optimized scroll technology. 2010, [Accessed 20 December 2023].
[27] Haglund Stignor C, Walfridson T. Nordsyn study on air-to-water heat pumps in humid nordic climate. In: Nordic council of ministers. 2019.
[28] Boverket. Energi i bebyggelsen – tekniska egenskaper och beräkningar– resultat från projektet BETSI. [Online]. Available: https://www.boverket.se/sv/om-boverket/publicerat-av-boverket/publikationer/2011/energi-i-bebyggelsen—tekniska-egenskaper-och-berakningar/.
[29] Hedbrant J. On the thermal inertia and time constant of single-family houses [Licentiate dissertation], Linköping: Linköpings Universitet; 2001, 2001.
[30] Energy Performance, SIS/TK 189/AG 05/. Energy performance of buildings — Part 1: Classification of power need for space heating. [Online]. Available: https://www.sis.se/produkter/byggnadsmaterial-och-byggnader/bygginstallationer/ovrigt/ss-24300-12020/.
[31] Statistics Sweden SCB. Just over 5.2 million dwellings in Sweden. 2025, [Accessed 20 November 2025].
[32] Purmo. Technical catalogue, panel radiators. [Online]. Available: https://www.purmo.com/docs/Purmo-technical-catalogue-full-panel-radiators-10_2021_EN.pdf.
[33] Daikin. Daikin altherma 3 GEO, Installer reference guide. [Online]. Available: https://www.daikin.eu/content/dam/document-library/Installer-reference-guide/heat/ground-to-water-heat-pump/EGSAH-D9W.EGSAX-D9W%28G%29_Installer%20reference%20guide_4PEN569820-1E_English.pdf.
[34] NIBE. Sustainable heat pumps for all homes. [Online]. Available: https://www.nibe.eu/en-eu/products/heat-pumps.
[35] CopelandTM. Emerson climate technologies. In: $copeland^{TM}$ scroll variable speed compressors for residential air conditioning applications. Emerson Electric Co.; 2020, [Online]. Available: https://climate.emerson.com/documents/product-brochure-copeland-scroll-variable-speed-compressors-for-residential-air-conditioning-applications-en-sg-7237218.pdf. [Accessed 04 March 2022].
[36] Energy Stats UK. Vaillant arotherm weather curve information. 2025, [Online]. Available: https://energy-stats.uk/vaillant-arotherm-weather-curve-information/. [Accessed 01 May 2025].
[37] Maivel M, Kurnitski J. Heating system return temperature effect on heat pump performance. Energy Build 2015;94:71–9.